

# Blueshift of intersubband magneto-optical transitions linked to void states of thin barriers in multiple quantum well structures

F. Carosella,<sup>1</sup> R. Ferreira,<sup>1</sup> G. Strasser,<sup>2</sup> K. Unterrainer,<sup>3</sup> and G. Bastard<sup>1,3,4</sup>

<sup>1</sup>*Laboratoire Pierre Aigrain, Ecole Normale Supérieure, CNRS UMR 8551, Université P. et M. Curie, Université Paris Diderot, 24 rue Lhomond, F-75005 Paris, France*

<sup>2</sup>*Solid State Electronics Institute, Technical University Vienna, Floragasse 7, A-1040 Vienna, Austria*

<sup>3</sup>*Photonics Institute, Technical University Vienna, Gusshausstr. 25-29, A-1040 Vienna, Austria*

<sup>4</sup>*Wolfgang Pauli Institut c/o Fak. f. Mathematik, Univ. Wien-UZA 4, Nordbergstrasse 15, A-1090 Vienna, Austria*  
(Received 27 May 2010; published 30 July 2010)

We show by numerical diagonalization that the presence of interface defects leads to a small low-energy redshift of the intersubband magnetoabsorption in single quantum wells but to a large blueshift in double quantum wells with very thin intermediate barrier. The blueshift is associated with states that localize around voids in the thin defective barrier.

DOI: [10.1103/PhysRevB.82.033307](https://doi.org/10.1103/PhysRevB.82.033307)

PACS number(s): 73.21.Ac, 78.67.Pt

In the search of THz absorbing or emitting devices, it often happens that a wide single quantum well (SQW) is split into two (or more) by inserting one (or several) very thin (one or a few monolayers) barrier(s) in the vicinity of the center of the wide SQW. It becomes effectively a double (or triple, or more) well (DQW, TQW, etc., with a very strong tunnel coupling between the wells. Placing a repulsive potential near the center of the wide well allows decreasing the energy  $E_2 - E_1$  of the ground intersubband transition<sup>1</sup> in a controllable fashion. However, to our knowledge, the importance of interface defects of thin intermediate barriers on the device behavior has not been fully realized. The effects of interface defects on intersubband absorption or emission (at magnetic field  $B=0$  or  $B \neq 0$ ) are usually taken into account by means of a level lifetime or by accounting for an inhomogeneous broadening. Both procedures amount essentially to rounding off the delta function of the energy conservation in the intersubband line shape.<sup>2-7</sup> Exact diagonalization of lateral disorder has also been tackled at  $B=0$  for the study of the intersubband<sup>8</sup> and interband<sup>9,10</sup> transitions of a SQW. In the specific case of interface defects of very thin barriers [ideally monolayer (ML) barriers] the interface defects are voids in these barriers, thereby allowing the existence of laterally confined electron states for which the barrier simply does not exist. Under such a circumstance, for the electrons in these void states the sample is no longer a DQW but a broad SQW with an intersubband transition energy that markedly differs from the ideal DQW one. To directly probe the voids states requires a taylorable lateral confinement. A strong magnetic field applied parallel to the growth axis of the DQW structure provides it. We note that a strong magnetic field is known to significantly alter the output power of quantum cascade lasers (QCL).<sup>6,7,11-13</sup> Together with the improvement of the laser performance, shifts of the lasing transitions are often observed.<sup>12,13</sup> Here, we would like to point out a possible origin of these shifts, namely, the unavoidable existence of interface defects.

We shall establish in this work that the laterally confined void states affect very strongly the optical response of DQW based emitters or absorbers. We shall first show that the interface defects always induce a small low-energy redshift of

the  $E_1 \rightarrow E_2$  absorption in a SQW. We shall then demonstrate that the void states in a DQW have a distinct optical signature since they lead to a large blueshift of the ground intersubband absorption when the temperature  $T$  decreases or  $B$  increases, in striking contrast with the SQW case.

We consider either a SQW or a DQW with two wells separated by a thin barrier. A strong magnetic field is applied parallel to the  $z$  direction. The vector potential is taken as  $\vec{A} = (0, Bx, 0)$ . We work in the envelope function approximation, that is known to be accurate even in short period GaAs/AlAs superlattices.<sup>14</sup> The hamiltonian reads

$$H = H_0 + V_{\text{def}}(\vec{r}),$$

$$H_0 = \frac{p_x^2}{2m^*} + \frac{(p_y + eBx)^2}{2m^*} + \frac{p_z^2}{2m^*} + V_{\text{SQW/DQW}}(z),$$

$$V_{\text{def}}(\vec{r}) = V_b \sum_{j, \vec{\rho}_{i(j)}} \text{sign}(i, j) \exp\left\{-\frac{[\vec{\rho} - \vec{\rho}_{i(j)}]^2}{2\sigma^2}\right\} F_{j,i}(z). \quad (1)$$

In Eq. (1)  $V_{\text{SQW/DQW}}$  is the  $z$ -dependent potential profile of the ideal SQW/DQW and  $V_b$  is the barrier height.  $V_{\text{def}}$  is the potential energy due to the interface defects. It is modeled by a sum of  $N_{\text{def},j}$  Gaussian potentials located at random sites  $\vec{\rho}_{i(j)}$  in the layer plane for the  $j$ th interface. In Eq. (1),  $\text{sign}(j, i)$  is  $-1$  when the well protrudes in the barrier and  $+1$  in the opposite case, and  $F_{j,i}(z)$  define the  $z$  region where the defect at  $\vec{\rho}_{i(j)}$  is placed. For instance, if the  $j$ th ideal interface is at  $z = z_j$  and corresponds to a well (barrier) at  $z > z_j$  ( $z < z_j$ ), for an attractive or repulsive defect of thickness there is  $F_{ji}^{\text{attractive}}(z) = \theta[z - (z_j - h)]\theta[z_j - z]$  and  $F_{ji}^{\text{repulsive}}(z) = \theta[z - z_j]\theta[(z_j + h) - z]$ .

The sites  $\vec{\rho}_{i(j)}$  are taken uncorrelated as well as their distribution on the interfaces. The number of defects of a given interface is specified in terms of an effective coverage of the surface  $S$ :  $\text{fr} = N_{\text{def},j} \pi \sigma^2 / S$ . Moreover, we ensure that the total (i.e., for all interfaces) number of attractive and repulsive defects gives a zero average for the diagonal matrix elements of the defect potential  $V_{\text{def}}^l(\vec{\rho})$  ( $l$  is the subband index, see below). In the numerical calculations, we take for all struc-

tures:  $\sigma=10.8$  nm,  $\text{fr}=0.15$  for all interfaces, a finite sample area of  $200\text{ nm}\times 200\text{ nm}$ , the material parameters for GaAs/AlGaAs QWs ( $V_b=0.393$  eV, effective masses  $m^*=0.07m_0$  in the wells and  $m^*=0.124m_0$  in the barriers, and  $a_{\text{ML}}=0.283$  nm for the ML thickness), and one ML defects ( $h=a_{\text{ML}}$ ). Finally, for the intermediate barrier of the DQW structure, the repulsive defects are placed only at the left interface.

The defect potential has been diagonalized on the basis where  $H_0$  is diagonal. In addition, since the defect potential is weak, the mixings between different subbands were disregarded. Intrasubband inter-Landau levels (LL) mixings were considered for completeness. We found that they do not provide much difference compared to the situation where we retain a single Landau level in the basis (except to induce optical transitions that are optically forbidden). The particular resonant fields, where two LL's belonging to different subbands cross, were avoided. Under such circumstances, for a given subband  $l$  the defect potential becomes quasi-two-dimensional (2D). For instance,

$$V_{\text{def}}^l(\vec{\rho}) = \sum_j \lambda_{l,j} \sum_{\vec{\rho}_{i(j)}} \exp\left\{-\frac{[\vec{\rho} - \vec{\rho}_{i(j)}]^2}{2\sigma^2}\right\},$$

$$\lambda_{l,j} = V_b \int_{z_j}^{z_{j+h}} \chi_l^2(z) dz, \quad (2)$$

where the specific case of repulsive defects sitting on the barrier/well interface at  $z_j$  has been considered and where  $\chi_l(z)$  is the wave function corresponding to the  $E_j$  subband. This is this effective in-plane potential that lifts the degeneracy of the unperturbed LL.

An unperturbed SQW or DQW admits strict optical selection rules for intersubband magneto-optical transitions. Only transitions that conserve the LL index as well as the center of the orbits are allowed if the electromagnetic wave is polarized along the  $z$  direction. Since the LL mixing plays a small part, we shall examine separately the effect of the defects on the states with the same LL index but related to different subbands. The intersubband absorption is proportional to

$$\alpha(\omega) \propto \sum_{\nu,\mu} f(\varepsilon_{E_l,0,\mu}) |\langle E_2, n=0, \nu | z | E_1, n=0, \mu \rangle|^2 \times \delta(E_2 - E_1 + \varepsilon_\nu - \varepsilon_\mu - \hbar\omega), \quad (3)$$

where  $\langle \vec{r} | E_l, n, \nu \rangle = \chi_l(z) \psi_{\nu(l,n)}(\vec{\rho})$  denotes the wave function of the  $\nu$ th state of the  $n$ th broadened LL of the  $l$ th subband with energy  $\varepsilon_{l,n,\nu} = E_l + (n+1/2)\hbar\omega_c + \varepsilon_{\nu(l,n)}$ .  $f(\varepsilon_{1,0,\mu})$  is the statistical occupation of the available initial states. Since we consider systems with few electrons,  $f(\varepsilon_{1,0,\mu})$  can be approximated by a Boltzmann factor corresponding to a temperature  $T$ .

The numerical calculations imply an average over different configurations of the disorder. Thus, for a given disorder realization, we compute the energy levels, wave functions, and optical absorption. Another realization with the same coverage  $N_{\text{def},j}$  is made and the calculations are repeated. Altogether, the calculations were repeated for 100 different configurations of the interface defects. An average over the

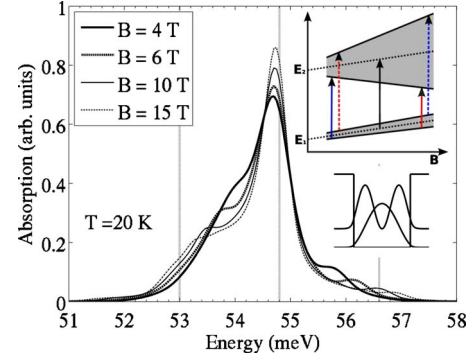


FIG. 1. (Color online) Calculated absorption spectrum of the SQW at different magnetic fields and  $T=20$  K. The upper inset panel depicts the field evolution of the independently broadened LLs. The gray zones indicate that the excited LL is much broader than the ground one because of its larger probability of presence near the disordered interfaces (lower inset panel). The solid (dashed) arrows show that transitions involving correlated states at low (high) energy tail redshift (blueshift) with increasing  $B$ , as compared to the  $B$ -independent transition in absence of disorder (bold central arrow).

100 absorption spectrum obtained leads to the final spectra that are discussed below. In the following we discuss the  $B$  and  $T$  variations in the absorption spectrum of two structures: a SQW of thickness  $L_z=2L_{z0}+a_{\text{ML}}$  with  $L_{z0}=7$  nm and a DQW  $L_{z0}/a_{\text{ML}}/L_{z0}$  DQW of same total thickness but with a very thin (1-ML-thick) intermediate barrier.

In the SQW case, the interface defects play a minor part in the broadening. This is illustrated in Fig. 1 where we show the calculated absorption line shape versus photon energy at  $T=20$  K and different values of  $B$ . For the nominal QW, the absorption is a  $B$ - and  $T$ -independent line centered at the unperturbed energy  $\Delta E_{\text{SQW}}=E_2-E_1=54.8$  meV. In the presence of defects, the absorption spectrum contains additional contributions, which are related to different configurations of defects involving the two interfaces. Indeed, the vertical bars in Fig. 1 locate the transition energies for a SQW with nominal width (54.8 meV) or 1 ML thicker (53 meV) or thinner (56.6 meV). However, the prominent feature in Fig. 1 is a redshift (blueshift) of the low-energy (high-energy) defect-related wings with increasing  $B$ . In order to interpret these findings, let us consider initially only one interface of the SQW. The effective 2D potentials in Eq. (2) are the same for  $E_2$  and  $E_1$  apart from the multiplicative factor  $\lambda_{l,1}$ .<sup>15</sup> Owing to this peculiar situation, the two ensembles of independently disordered states  $\{\varepsilon_{\nu(l,n)}; \Psi_{\nu(l,n)}(\vec{\rho})\}$  ( $\nu=1, 2, \dots; n=0; l=1$  or  $2$ ) can easily be shown to display two characteristics: (i) their energies are spectrally correlated:  $\varepsilon_{\nu(l=1,n)}/\lambda_{1,1} = \varepsilon_{\nu(l=2,n)}/\lambda_{2,1}$  and (ii) their in-plane motions are identical:  $\Psi_{\nu(l=1,n)}(\vec{\rho}) = \Psi_{\nu(l=2,n)}(\vec{\rho})$ . This strong spectral and spatial correlation has deep consequences on the optical properties. First, it follows straightforwardly from (i) that the excited subband  $E_2$  is more affected (and thus broader) than the ground one  $E_1$ , just because the effective 2D potential is deeper in  $E_2$  than in  $E_1$  ( $\lambda_{2,1} > \lambda_{1,1}$ ). Note that the actual broadening value, which can only be obtained by solving Eq. (1), increases as expected<sup>16</sup> with increasing  $B$  (as depicted by the gray areas

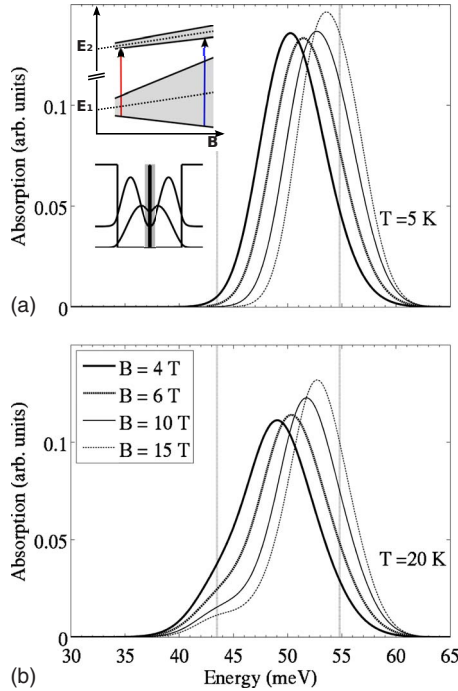


FIG. 2. (Color online) Calculated absorption spectrum of the DQW at different magnetic fields and (a)  $T=5$  K and (b) 20 K. The upper inset panel in (a) depicts the field evolution of the independently broadened LLs. The gray zones indicate that the ground LL is much broader than the excited one because of its larger probability of presence near the intermediate thin barrier (lower inset panel). The arrows show that transitions involving correlated states at low  $T$  blueshift with increasing  $B$ .

in the inset of Fig. 1). Second, because of (ii), the dipole matrix element in Eq. (3) is nonzero only if  $\mu = \nu$ , irrespective of the nature of the eigenstates (localized or extended). At low temperature and strong magnetic field the electrons get localized at the local minima of a given realization of the disorder. Because of (i), a local minimum introduces a low-energy tail state in both  $E_1$  and  $E_2$  sets of broadened LL states. Hence, altogether, the freeze out of electrons on the lowest lying states of the ground subband, joined to the spectral and spatial correlation effects, and the increase of the LL broadenings with  $B$ , imply that the low-energy wing of the optical spectrum presents a redshift that increases when  $T$  decreases or  $B$  increases (see arrows in the inset of Fig. 1). Similar reasoning explains the blueshift of the high-energy absorption wing (its weaker intensity is due to thermal occupancy of high-energy tail states in the initial subband). Now, in actual samples, there are several interfaces. This in principle invalidates the exact proportionality between the effective potentials in  $E_1$  and  $E_2$ . However, we have checked that for the tail states the dipole matrix elements in Eq. (3) are important only when the localization centers of the  $\mu$  and  $\nu$  states are close (in other words the transitions are quasidiagonal in real space, as already noticed in Ref. 8 at  $B=0$ ).

The absorption in a DQW with thin intermediate barrier displays a completely different behavior. This is illustrated in Fig. 2 where we show the absorption lineshape at different fields and temperature. The ideal DQW has a  $B$ - and  $T$ -independent intersubband transition at the energy  $\Delta E_{\text{DQW}}$

$=43.5$  meV (vertical bar in Fig. 2). This intrinsic line is practically absent (5 K) or only marginally present (20 K) in the presence of defects. Indeed, Fig. 2 shows that the presence of defects leads to an important blueshift for the DQW absorption peak, which increases when  $T$  decreases or  $B$  increases. This is in striking contrast with the modest shifts calculated for a SQW. This intriguing behavior can nevertheless also be explained with the help of the same model of spectral and spatial correlations used for SQW. Note initially that in a DQW one can rule out the outer well/barrier interfaces because as for a regular single well the probability distribution is very small at those interfaces. As depicted in the inset of Fig. 2(a), the wave function of the ground (the excited) subband of a DQW has a maximum (a node) at the DQW center. As a result, the ground (excited) subband is very strongly (only weakly) affected by defects in the 1-monolayer-thick intermediate barrier ( $\lambda_{2,1} \ll \lambda_{1,1}$ ).

Thus, in striking contrast with what happens in SQW, the  $n=0$  LL will be broader for  $E_1$  than for  $E_2$  (see gray areas in the inset of Fig. 2). Finally, similar reasoning using the freezing out of electrons at low  $T$  and high  $B$  as well as the eigenstates correlation effects, as done for the SQW case, allows explaining the calculated blueshifts for the intersubband DQW absorption (see arrows in the inset of Fig. 2). We have calculated the ratios  $\lambda_{1(\text{SQW})}:\lambda_{2(\text{SQW})}:\lambda_{1(\text{DQW})}:\lambda_{2(\text{DQW})} \approx 8:28:110:1$ , what explains the much larger blueshift in DQW as compared to the SQW ones.

For the central thin barrier of a DQW it is important to realize that an interface defect (which should be at least 1-monolayer-thick) means a void. If now  $B$  is large enough so that the cyclotron radius  $l = (\hbar/eB)^{1/2}$  is smaller than the defect radius, there will exist localized electron states at lower energies, as compared to the ideal DQW, where the carrier is trapped. The carrier occupying such localized states feels the spatial  $z$  localization of the broader SQW, for which the  $E_2$  to  $E_1$  transition energy is higher ( $\Delta E_{\text{SQW}} = 54.8$  meV; see vertical bar in Fig. 2). This situation is favored at low temperature and high field because, in the  $E_1$  subband, being in a void means a substantial decrease in the electron energy. Note that even though the number of voids represents only a small fraction of the total number of states, this smallness is offset by the Boltzmann factor at low temperature. Hence, the dominant absorption peak comes from the voids. At elevated temperature the more numerous unperturbed regions starts playing a larger role compared to the voids and the dominant absorption peak shifts toward lower energies heading to the position of the unperturbed DQW at 43.5 meV.

It is worth pointing out that similar voids states exist at zero magnetic field. In fact, one can easily construct a Gaussian wave packet out of plane waves that will be localized around a given void and will have an in plane extension smaller than the defect size. Even without counting the potential energy gain, the thermal excitation [ $k_B T_\alpha \approx \hbar^2 \alpha^2 / (2m^*)$ , where  $\alpha = \sigma^{-1}$  is the in-plane wave-vector extension of the wave packet) will make the void states operative in the optical response. We note that the voids states may be very detrimental to the lasing action of QCL at the nominal lasing energy to the extent that carrier in such states do not participate to the amplification of the laser field.

In conclusion, we point out that the insertion of thin bar-

riers inside a broad quantum well not only changes the energy level of the ideal structure (thereby allowing to adjust the intersubband transition energy) but has very deep effects on the absorption (or emission) line shape that have so far been unforeseen. First, because any interface has defects, the presence of the thin barrier induces a very efficient trapping of the electrons on these defects, thereby distorting the line shape considerably. We have shown that, in contrast to single QW where the trapping induces small redshift of the inter-LL transition, the trapping on the defects of a thin barrier induces a pronounced blueshift of this transition. In addition, when a strong magnetic field is applied parallel to the growth axis it induces a spectacular magnetic freeze out of the electrons on the interface defects that leads to a further blueshift of the intersubband transition. The controllable in-plane localization brought by the magnetic field allows the creation

of particular electron states for which the electron moves as if the central barrier does not exist. These states have low energies and are therefore dominant in the absorption (or emission) line shapes at low temperature. Additionally, voids states of different subbands display strong spectral and spatial correlations, which control both their energetic distribution and dipolar coupling. Accounting for their existence in terahertz quantum cascade structures, where the carrier concentration is low, may give a clue to better understand the behavior of these structures and to better ascertain the part played by the interface defects.

The LPA-ENS is UMR 8551 CNRS associated with the Universities Paris 6 and Paris 7. One of us (G.B.) is pleased to acknowledge the financial support of the Wolfgang Pauli Institute and TUWien.

- 
- <sup>1</sup>For a review on intersubband transitions see *Intersubband Transitions in Quantum Wells: Physics and Devices Applications*, Semiconductors and Semimetals Vol. 62, edited by H. C. Liu and F. Capasso (Academic Press, San Diego, 2000).
- <sup>2</sup>T. Unuma, M. Yoshita, T. Noda, H. Sakaki, and H. Akiyama, *J. Appl. Phys.* **93**, 1586 (2003).
- <sup>3</sup>T. Unuma, N. Sekine, and K. Hirakawa, *Appl. Phys. Lett.* **89**, 161913 (2006).
- <sup>4</sup>C. C. Phillips, E. A. Johnson, R. H. Thomas, H. L. Vaghjiani, I. T. Ferguson, and A. G. Norman, *Semicond. Sci. Technol.* **8**, S373 (1993).
- <sup>5</sup>J. B. Khurgin, *Appl. Phys. Lett.* **93**, 091104 (2008).
- <sup>6</sup>C. Becker, A. Vasanelli, C. Sirtori, and G. Bastard, *Phys. Rev. B* **69**, 115328 (2004).
- <sup>7</sup>A. Leuliet, A. Vasanelli, A. Wade, G. Fedorov, D. Smirnov, G. Bastard, and C. Sirtori, *Phys. Rev. B* **73**, 085311 (2006).
- <sup>8</sup>C. Metzner, M. Hofmann, and G. H. Döhler, *Phys. Rev. B* **58**, 7188 (1998).
- <sup>9</sup>V. Savona, in *Electron and Photon Confinement in Semiconductor Nanostructures*, edited by B. Deveaud, A. Quattropani, and P. Schwendimann (IOS Press, Amsterdam, 2003).
- <sup>10</sup>E. Runge, in *Solid State Physics*, edited by H. Ehrenreich and F. Spaepen (Academic Press, San Diego, 2002), Vol. 57, pp. 149–305.
- <sup>11</sup>C. Scalari, C. Walther, L. Sirigu, M. L. Sadowski, H. Beere, D. Ritchie, N. Hoyler, M. Giovannini, and J. Faist, *Phys. Rev. B* **76**, 115305 (2007).
- <sup>12</sup>V. Tamosiunas, R. Zobl, J. Ulrich, K. Unterrainer, R. Colombelli, C. Gmachl, F. Capasso, K. West, and L. Pfeiffer, *Appl. Phys. Lett.* **83**, 3873 (2003).
- <sup>13</sup>A. Wade, G. Fedorov, D. Smirnov, S. Kumar, B. S. Williams, Q. Hu, and J. L. Reno, *Nat. Photonics* **3**, 41 (2009).
- <sup>14</sup>G. Bastard, J. A. Brum, and R. Ferreira, in *Solid State Physics Advances in Research and Applications*, edited by H. Ehrenreich and D. Turnbull (Academic Press, San Diego, 1991), Vol. 44, p. 229.
- <sup>15</sup>This property is exact if  $\int_{z_0}^{z_0+h} \chi_n^2(z) dz = \int_{z_0-h}^{z_0} \chi_n^2(z) dz$ . This is nearly true in our material system. For instance, in the  $L_{z0}/a_{ML}/L_{z0}$  DQW the two integrals calculated on the right side and on the left side of the intermediate barrier, for the first subband  $E_1$ , are 3.39% and 3.27%, respectively.
- <sup>16</sup>T. Ando, A. B. Fowler, and F. Stern, *Rev. Mod. Phys.* **54**, 437 (1982).